HOW SPECIAL ARE DARK GAMMA-RAY BURSTS: A DIAGNOSTIC TOOL

EVERT ROL,[1,2,3,4] RALPH A. M. J. WIJERS,[3] CHRYSSA KOUVELIOTOU,[4,5] LEX KAPER,[3] AND YUKI KANEKO[6]

ABSTRACT

We present here a comprehensive study of the optical/near-infrared (IR) upper limits for gamma-ray bursts that have an X-ray afterglow. We have extrapolated the X-ray afterglows to optical wavelengths based on the physics of the fireball blast wave model and compared these results with optical upper limits for a large sample of bursts. We find a small set of only three bursts out of a sample of 20 for which the upper limits are not compatible with their X-ray afterglow properties within the context of any blast wave model. This sparse sample does not allow us to conclusively determine the cause of this optical/near-IR deficit. Extinction in the host galaxy is a likely cause, but high redshifts and different afterglow mechanisms might also explain the deficit in some cases. We note that the three bursts appear to have higher than average gamma-ray peak fluxes. In a magnitude versus time diagram the bursts are separated from the majority of bursts with a detected optical/near-IR afterglow. However, two gamma-ray bursts with an optical afterglow (one of which is highly reddened) also fall in this region with dark bursts, making it likely that dark bursts are at the faint end of the set of optically detected bursts, and therefore the dark bursts likely form a continuum with the bursts with a detected optical afterglow. Our work provides a useful diagnostic tool for follow-up observations for potentially dark bursts; applied to the events detected with the *Swift* satellite, it will significantly increase our sample of truly dark bursts and shed light upon their nature.

Subject headings: dust, extinction — gamma rays: bursts

Online material: machine-readable tables

1. INTRODUCTION

After the discovery of the first gamma-ray bursts (GRBs) (Klebesadel et al. 1973), it took nearly 30 years before emission at other wavelengths (afterglow) was discovered (Costa et al. 1997; van Paradijs et al. 1997; Frail et al. 1997) and the distance scale was determined (Metzger et al. 1997). We know today that the main reasons for this delay were the relatively rapid decay of the afterglows and the inaccuracy of the initial burst localizations: (optical) searches for afterglows have to be performed within 1 or 2 days after the burst has been triggered in gamma rays and before the afterglow flux level has decreased below the telescope detection limit. These searches have to be performed with large-aperture telescopes (requiring arcminute-sized error boxes) or with sufficiently long exposure times on smaller telescopes. Both options were rarely feasible for a long time, since either the delay between the occurrence of the GRB and the availability of its position was too large, or the size of the error box of the GRB was too large to perform efficient follow-up observations. The rapidly available and accurate positions provided initially by the Wide Field Cameras (WFCs) on board the Italian-Dutch *BeppoSAX* satellite, and later with *HETE-2*, combined with X-ray afterglow counterparts localized with the *BeppoSAX* Narrow Field Instruments (NFIs), *Chandra*, and *XMM-Newton*, made rapid follow-up observations at longer wavelengths possible, with a typical error circle diameter of the same order as the field of view of a large optical telescope.

It was noted very soon, however, that despite rapid follow-up and deep imaging, some bursts escaped the detection of an optical counterpart (e.g., Groot et al. 1998); these have been traditionally designated as "dark bursts." Notably, an optical afterglow was found in only 35% of the *BeppoSAX* bursts for which an X-ray (2–10 keV) afterglow was detected (see, e.g., De Pasquale et al. 2003). Interestingly, however, eight of 10 bursts recently detected with the soft X-ray camera (SXC) on board *HETE-2* have a detected optical or near-IR afterglow, increasing the detection rate to 80%. This discrepancy in their dark bursts rates reflects the current improvement of the community response in GRB alerts, as well as today's enhanced observational capabilities, rather than an intrinsic difference in the properties of the GRBs detected by the two satellites.

Several explanations have been brought forward to address the absence of detectable optical flux, apart from adverse observing conditions: dark bursts could be intrinsically faint at optical wavelengths (possibly reflecting a difference in their central engine from "normal" GRBs); they could be at high redshift, which would result in their optical/near-IR light being suppressed because of hydrogen (Lyα) absorption; or they could be heavily extincted by gas and dust. The latter would not be unexpected, since the afterglows are located close to the center of light of their host galaxy (Bloom et al. 2002a). Furthermore, it is known now that at least a subclass of GRBs originate from the core collapse of a massive star (Hjorth et al. 2003b; Stanek et al. 2003). Since these massive stars are very short-lived, they are expected not to travel far away from their birthplace, which is most likely a very dusty environment. There are cases, however, where the host galaxy shows a high column density of neutral hydrogen, as expected for massive-star progenitors, but where

[1] Department of Physics and Astronomy, University of Leicester, University Road, Leicester LE1 7RH, UK; er45@star.le.ac.uk.

[2] INAF–Osservatorio Astronomico di Trieste, Via Tiepolo 11, 34131 Trieste, Italy.

[3] Astronomical Institute, University of Amsterdam, Kruislaan 403, 1098 SJ Amsterdam, Netherlands; rwijers@science.uva.nl, lexk@science.uva.nl.

[4] Institute for Nuclear Theory, University of Washington, Seattle, WA 98195-1550.

[5] NASA/MSFC, SD-50, 320 Sparkman Drive, Huntsville, AL 35805; chryssa.kouveliotou@nasa.gov.

[6] University of Alabama, NSSTC, SD-50, 320 Sparkman Drive, Huntsville, AL 35805; yuki.kaneko@msfc.nasa.gov.

strong upper limits are set on the reddening (and thus the dust content) in the host galaxy, e.g., for GRB 020124 (Hjorth et al. 2003a) and for GRB 030323 (Vreeswijk et al. 2004). In such cases, it is possible that X-ray dust destruction might free the way for the afterglow radiation to be still detected (Fruchter et al. 2001).

It is important to note here that the current designation of a burst as "dark" may reflect either that no afterglow has been found by optical/near-IR searches, or that the optical counterpart is extremely faint initially and declines very rapidly, thus precluding detection when observed later than 1 day after the burst (see, e.g., Fynbo et al. 2001; Lazzati et al. 2002; Hjorth et al. 2002; Berger et al. 2002). In the present study, however, we define as "dark" bursts that fall below an upper limit in their afterglow flux, which we derive using the fireball model. In this physical definition of dark bursts, the input for our calculations is obtained from observations in other wavelengths (X-ray or radio) in which the afterglow was detected. Of course, if there is no detection at any wavelength, this definition is not applicable and one has to revert to the original empirical definition. Thus, to define our sample of "physically dark bursts," we have limited ourselves to those with a detected X-ray afterglow, from which we can predict the optical/near-IR fluxes.

The typical power-law decline of the X-ray and optical afterglows, as well as the afterglow broadband spectra obtained from observations at radio, millimeter, infrared, optical, and X-ray wavelengths, show that the standard fireball model proposed as an explanation for these phenomena (Rees & Mészáros 1992; Mészáros & Rees 1997; Wijers et al. 1997) is to a large extent acceptable. This standard model has been modified to account for the possible collimation of the outflow of the gamma-ray burst and its afterglow (e.g., Rhoads 1997, 1999) and for the expansion of the afterglow into a medium with a density gradient (e.g., a stellar wind; Chevalier & Li 1999). In general, the model can be constrained by the available observations of a GRB afterglow. On the other hand, if observations in a particular wavelength interval are missing, it is possible to use the afterglow model to predict the flux (as a function of time) in this wavelength regime, which is what we have done below. The outline of this paper is as follows. In § 2 we describe the method used to constrain the optical/near-IR magnitudes expected from the X-ray afterglows. The results are analyzed in § 3 and discussed in the context of the current ideas to explain dark bursts. Finally, we show how our results can be used as a diagnostic tool for future observations and studies of dark bursts.

2. THE METHOD

2.1. *X-Ray Measurements*

We have collected the X-ray afterglow observations from various sources (refereed journals, proceedings, GCN circulars) and obtained a total of 20 X-ray afterglows with no optically detected burst, as well as one X-ray afterglow for an optically faint burst (GRB 020322). The available X-ray fluxes were first converted to the frequency corresponding to the observed energy-band logarithmic average, instead of the usually quoted flux in the 2–10 or 0.2–10 keV range. This was done using, for example, $F_{2-10} = \int_2^{10} F_{av} \times (E/E_{av})^\beta \, dE$, where β is the energy spectral index, E_{av} is the logarithmic average, and F_{av} is the corresponding flux (e.g., for the 2–10 keV interval, $E_{av} = 5$ keV). Since the quoted fluxes are generally an average of the flux in the observed time interval, we interpolated the flux to a logarithmic average t_{av} using the temporal decay index δ in a similar way. The choice of

this spectral and temporal average ensures that our fluxes are not heavily dependent on the power-law indices β and δ.

In cases where no spectral index was reported, we have assumed a Crab-like spectrum. The error induced by this assumption is generally small because of the choice of the logarithmic average as our pivot energy: for example, for an F_{2-10} flux of 5×10^{-9} ergs cm^{-2} s^{-1} and β between 0.6 and 1.4, the F_5 flux varies only between 5.8×10^{-10} and 6.4×10^{-10} ergs cm^{-2} s^{-1} keV^{-1}. We have assumed a 20% error in the flux and the temporal or spectral indices of the X-rays if no error was listed. Table 1 lists the X-ray afterglows that have been used in our analysis.

2.2. *Optical Data*

Optical and near-IR data were largely obtained from the GCN circulars, with additions from refereed journals and conference proceedings. The *R*-band upper limit for GRB 000214 was obtained during our observing program on the 2.2 m ESO telescope at the La Silla observatory. The data were reduced in a standard fashion and calibrated using a set of Landolt standard stars.

All optical and near-IR magnitudes have been corrected for Galactic extinction using the *COBE* DIRBE maps (Schlegel et al. 1998). Corrected magnitudes have been converted to fluxes using the Vega flux values provided by Fukugita et al. (1995) for optical magnitudes and those by Beckwith et al. (1976) for infrared observations.

Where the quoted upper limit was the Digitized Sky Survey (e.g., "we find no new sources down to the limit of the DSS"), we have assumed a limiting magnitude of 20. Unfiltered observations were left out of the analysis, unless the authors have given a corresponding filter and magnitude. Table 2 lists the upper limits that we have used for comparison with the X-ray afterglows. This list has been compiled by using the strongest upper limits available for a specific burst. Also, for the more recent bursts, currently only reports in GCN and IAU circulars exist, which should be considered temporary (this of course may be true for several of the older bursts as well).

2.3. *Predicting the Optical Flux by Extrapolating the X-Ray Afterglows*

We extrapolated the X-ray afterglow to the epoch and wavelength of the available optical and near-IR upper limits as follows. We first obtained a range of power-law indices p of the electron energy distribution from the 1 σ extremes of the X-ray power-law temporal and spectral indices. To do this, we assumed eight cases in the standard afterglow model, which were derived from a combination of the following: the cooling frequency ν_c was above or below the X-rays, the epoch of the X-ray observation was before or after the jet break in the light curve, and the fireball was expanding into a constant or a stellar wind density medium. For convenience, we have listed these combinations and the dependence of δ and β on p in Table 3. Some of these cases were ruled out by the fact that the two electron indices, inferred from the X-ray δ and β values, respectively, are incompatible with each other. We did not, however, limit the allowed range of p to $p > 2$ (for $p \leq 2$, one needs to put a high-energy cutoff on the electron distribution; see, e.g., Panaitescu & Kumar 2001 or Bhattacharya 2001). From the obtained values for p, we extrapolated in each case the $+1$ and -1 σ X-ray flux to the epoch and frequency of the optical/near-IR upper limit. For this extrapolation, we chose the extreme possibilities, such as placing the cooling frequency at either the optical frequency or at the X-ray frequency, or the epoch of the jet break right before or after the

TABLE 1
OVERVIEW OF X-RAY AFTERGLOWS OF BURSTS WITH OPTICAL NONDETECTIONS

Burst	Δt (days)	Flux (10^{-8} Jy)	δ	β	$p_{\min}-p_{\max}$	References
GRB 970402	0.620	$0.69^{+0.13}_{-0.19}$	$1.57^{+0.03}_{-0.03}$	$0.70^{+0.60}_{-0.60}$	1.54–3.13	1, 2
GRB 970828	1.571	$0.99^{+0.23}_{-0.22}$	$1.44^{+0.07}_{-0.07}$	$1.60^{+0.20}_{-0.30}$	2.60–2.68	3
GRB 971227	0.723	$0.75^{+0.15}_{-0.16}$	$1.12^{+0.08}_{-0.05}$	$1.10^{+0.22}_{-0.22}$	2.09–2.27	4
GRB 980613	0.458	$1.20^{+0.49}_{-0.50}$	$1.19^{+0.17}_{-0.17}$	$1.10^{+0.22}_{-0.22}$	2.03–2.81	5
GRB 981226	0.928	$1.30^{+1.10}_{-1.10}$	$1.31^{+0.44}_{-0.39}$	$0.92^{+0.47}_{-0.47}$	0.92–2.78	6
GRB 990704	0.660	$1.40^{+0.07}_{-0.13}$	$1.31^{+0.26}_{-0.26}$	$0.69^{+0.60}_{-0.34}$	1.05–2.58	7
GRB 990806	0.695	$0.73^{+0.20}_{-0.25}$	$1.15^{+0.03}_{-0.03}$	$1.16^{+0.50}_{-0.61}$	1.12–2.57	8
GRB 991014	0.852	$0.91^{+0.10}_{-0.12}$	$1.00^{+0.20}_{-0.20}$	$0.53^{+0.25}_{-0.25}$	0.80–2.56	9
GRB 000210	0.458	$2.30^{+0.45}_{-0.46}$	$1.38^{+0.03}_{-0.03}$	$0.95^{+0.15}_{-0.15}$	2.80–2.88	10
GRB 000214	0.923	$0.17^{+0.05}_{-0.05}$	$1.41^{+0.03}_{-0.03}$	$1.20^{+0.30}_{-0.30}$	2.51–2.92	11
GRB 000528	0.729	$0.25^{+0.06}_{-0.07}$	$1.33^{+0.13}_{-0.13}$	$0.95^{+0.19}_{-0.19}$	2.27–2.95	12
GRB 000615	0.880	$0.47^{+0.10}_{-0.11}$	$1.10^{+0.22}_{-0.22}$	$1.10^{+0.22}_{-0.22}$	1.84–2.43	13
GRB 001025A	2.078	$0.28^{+0.08}_{-0.13}$	$3.00^{+1.90}_{-1.90}$	$1.50^{+0.47}_{-0.12}$	2.76–4.90	14
GRB 001109	0.458	$11.00^{+3.30}_{-2.70}$	$2.40^{+0.48}_{-0.48}$	$1.26^{+0.12}_{-0.49}$	1.92–2.76	15
GRB 010214	0.458	$1.50^{+0.27}_{-0.64}$	$2.10^{+1.00}_{-0.60}$	$0.30^{+0.80}_{-0.60}$	1.50–3.20	15, 16
GRB 010220	0.829	$0.12^{+0.00}_{-0.07}$	$1.20^{+1.00}_{-1.00}$	$1.10^{+1.00}_{-0.60}$	1.00–3.93	14
GRB 011030	10.726	$0.59^{+0.03}_{-0.03}$	$2.10^{+0.60}_{-0.60}$	$0.31^{+0.08}_{-0.08}$	1.50–1.78	17
GRB 020321	0.742	$0.75^{+0.37}_{-0.40}$	$1.20^{+0.24}_{-0.24}$	$1.10^{+0.22}_{-0.22}$	1.95–2.92	18
GRB 020322[a]	0.751	$2.60^{+0.16}_{-0.18}$	$1.26^{+0.23}_{-0.23}$	$1.06^{+0.08}_{-0.08}$	2.04–2.28	19
GRB 020427	9.164	$0.27^{+0.03}_{-0.06}$	$2.30^{+0.60}_{-0.60}$	$0.30^{+0.20}_{-0.20}$	1.70–2.00	17
GRB 040223	0.393	$1.1^{+0.3}_{-0.3}$	$1.0^{+0.2}_{-0.2}$	$1.8^{+0.2}_{-0.2}$	[b]	20

NOTES.—We have also indicated the minimum and maximum values of the electron index p, which correspond to the minimum and maximum extrapolations in Fig. 1, respectively. Table 1 is also available in machine-readable form in the electronic edition of the *Astrophysical Journal*.

[a] Optically detected burst. See § 3 for details.

[b] The values for δ and β are incompatible with each other within the variants of the fireball model used in this paper, yielding no possible range for p.

REFERENCES.—(1) Nicastro et al. 1998; (2) Piro et al. 1997; (3) Yoshida et al. 2001; (4) Antonelli et al. 1999; (5) Costa et al. 1998; (6) Frontera et al. 2000; (7) Feroci et al. 2001; (8) Montanari et al. 2001; (9) in 't Zand et al. 2000; (10) Piro et al. 2002; (11) Antonelli et al. 2000; (12) Frontera 2003; (13) Nicastro et al. 2001; (14) Watson et al. 2002b; (15) De Pasquale et al. 2003; (16) Guidorzi et al. 2003; (17) Levan et al. 2005; (18) in 't Zand et al. 2004; (19) Watson et al. 2002a; (20) Tiengo et al. 2004.

epoch of the X-ray detection. In this way, we obtain the maximum and minimum values at optical/near-IR frequencies of the extrapolated X-ray afterglow. Sometimes such an extrapolation is ruled out by the standard afterglow model and the result is ignored. This happens, for example, when ν_c reaches ν_x when extrapolating back in time, while p was derived from the case where $\nu_x < \nu_c$.

By choosing the lowest and highest extrapolated flux, we obtain the flux range in which one would expect an optical counterpart to be found. Any upper limit *above* this range cannot be used to constrain the brightness of the optical afterglow. Any upper limit *below* this flux range will define this burst as physically "dark." Upper limits found within the flux range will be called "gray," and are subject to further study. Of course, the optical afterglow of gray bursts could very well be below the extrapolation of the X-ray afterglow, but so far there is no observational evidence supporting this assumption.

In some cases, the electron index p inferred from the available spectral and temporal index reached a value below 2. Since this index is generally found to be >2 for detected optical afterglows (but see some of the results of Panaitescu & Kumar [2001], who find indices of $p \approx 1.5$ for some afterglows), we have also calculated the lowest possible extrapolation with p fixed at 2. In most cases, however, the $p = 2$ extrapolation is well below the lowest minimum extrapolation from the available indices.

In the case of GRB 040223, a potential dark burst, the temporal and spectral indices of the X-ray afterglow (Tiengo et al. 2004) are incompatible with each other within the fireball model used here. We have listed the X-ray properties in Table 1, but we have not extrapolated the X-ray flux to the optical waveband.

3. RESULTS

In Figure 1 we show the results of the X-ray extrapolations and the various available upper limits at optical and near-IR wavelengths. For each X-ray afterglow, we only show the strongest optical and/or near-IR upper limit, as well as the minimum and maximum temporal extrapolation of the -1 and $+1$ σ X-ray flux to the frequency of the upper limit (*solid lines*). The dashed line is the extrapolation in the case $p = 2$, obtained for the -1 σ X-ray flux and the minimum temporal and spectral extrapolation.

There are only three GRBs out of the sample of 20 that we have found to be physically dark in this classification scheme: GRB 970828, GRB 000210, and GRB 001025A. Two of these bursts have already been noted to be dark by extrapolation of the available X-ray measurements (GRB 970828 [Groot et al. 1998] and GRB 000210 [Piro et al. 2002]).

In Table 4 we have indicated the dark bursts, together with the minimum amount of extinction (expressed in magnitudes) needed in the observer frame to explain the nondetection of the source.

We have also plotted R-band magnitudes for all available afterglows together with all R-band upper limits in a magnitude versus time diagram (time being the delay between the GRB trigger and the observation; Fig. 2), and indicated which upper limits

TABLE 2
Overview of Optical/Near-IR Upper Limits with X-Ray Afterglow Data Available

Burst	Filter	Δt (days)	Magnitude (uncorrected)	$E(B-V)$	Reference
GRB 970402.............	R	0.770	21.00	0.24	1
GRB 970828.............	R	0.174	23.80	0.04	2
GRB 971227.............	R	0.561	21.50	0.01	3
GRB 981226.............	I	0.692	23.50	0.02	4
GRB 981226.............	R	0.412	23.00	0.02	5
GRB 990704.............	R	0.231	22.20	0.04	6
GRB 990806.............	B	0.667	25.20	0.04	7
GRB 990806.............	R	0.697	23.30	0.04	8
GRB 991014.............	R	0.467	23.10	0.27	9
GRB 991014.............	K	1.240	19.00	0.27	10
GRB 000210.............	R	0.686	23.50	0.02	11
GRB 000214.............	R	0.337	23.24	0.06	12
GRB 000214.............	K	1.350	18.10	0.06	13
GRB 000528.............	R	0.734	23.30	0.09	14
GRB 000615.............	R	0.188	21.50	0.02	15
GRB 000615.............	H	0.705	20.50	0.02	16
GRB 001025A..........	R	1.168	24.50	0.06	17
GRB 001109.............	R	0.375	20.90	0.04	18
GRB 001109.............	K	0.400	19.00	0.04	19
GRB 010214.............	R	0.893	23.50	0.05	20
GRB 010220.............	R	0.361	23.50	0.85	21
GRB 010220.............	K	0.974	17.10	0.85	22
GRB 011030.............	R	0.300	21.00	0.39	23
GRB 011030.............	K	0.520	19.00	0.39	24
GRB 011030.............	R	1.000	23.61	0.39	25
GRB 011030.............	V	42.905	27.6	0.39	26
GRB 020321.............	R	1.099	23.60	0.10	27
GRB 020322[a]............	R	0.329	23.26	0.08	28
GRB 020427.............	V	44.603	28.7	0.03	26

Note.—Table 2 is also available in machine-readable form in the electronic edition of the *Astrophysical Journal*.

[a] Optically detected burst. See § 3 for details.

References.—(1) Groot et al. 1997; (2) Groot et al. 1998; (3) Castro-Tirado et al. 1997; (4) Bloom et al. 1998; (5) Lindgren et al. 1999; (6) Rol et al. 1999; (7) Greiner et al. 1999; (8) Kemp et al. 1999; (9) Thorstensen et al. 1999; (10) Klose et al. 2003; (11) Gorosabel et al. 2000; (12) this paper; (13) Rhoads et al. 2000; (14) Palazzi et al. 2000; (15) Stanek et al. 2000; (16) Pian et al. 2000; (17) Fynbo et al. 2000; (18) Greiner et al. 2000; (19) Castro Cerón et al. 2004; (20) Rol et al. 2001; (21) Berger et al. 2001; (22) Li Causi et al. 2001; (23) Mohan et al. 2001; (24) Klose et al. 2001; (25) Rhoads et al. 2001; (26) Levan et al. 2005; (27) Salamanca et al. 2002; (28) Bloom et al. 2002b.

belong to the dark bursts. Upper limits in other bands with an available X-ray spectral index were converted to R-band magnitude following the same method as used in the X-ray extrapolations (i.e., the resulting R-band upper limit is the extrapolation with the least constraining magnitude). We have drawn a power law with temporal index $\alpha = -1.5$ passing through 25th magnitude at 2 days, which separates the three dark bursts from practically all detected afterglows. This power law is not based on any particular physical model, but merely serves as a guide in the diagram.

TABLE 3
Temporal (δ) and Spectral (β) Indices as a Function of the Electron Power-Law Distribution Index p in the Slow Cooling Case

Medium	$\nu > \nu_c$		$\nu < \nu_c$	
	$\delta(p)$	$\beta(p)$	$\delta(p)$	$\beta(p)$
Pre–jet break (isotropic):				
ISM ($\rho = $ constant)...........................	$(3p-2)/4$	$p/2$	$3(p-1)/4$	$(p-1)/2$
Stellar wind ($\rho \propto R^{-2}$)....................	$(3p-2)/4$	$p/2$	$(3p-1)/4$	$(p-1)/2$
Post–jet break (collimated):				
ISM ($\rho = $ constant)...........................	p	$p/2$	p	$(p-1)/2$
Stellar wind ($\rho \propto R^{-2}$)....................	p	$p/2$	p	$(p-1)/2$

Notes.—Indices compiled for eight different scenarios (see, e.g., Sari et al. 1998 and Chevalier & Li 1999). We have chosen δ and β in such a way that they are positive in optical and X-rays for positive p; i.e., the afterglow flux follows $F(\nu, t) \propto \nu^{-\beta} t^{-\delta}$.
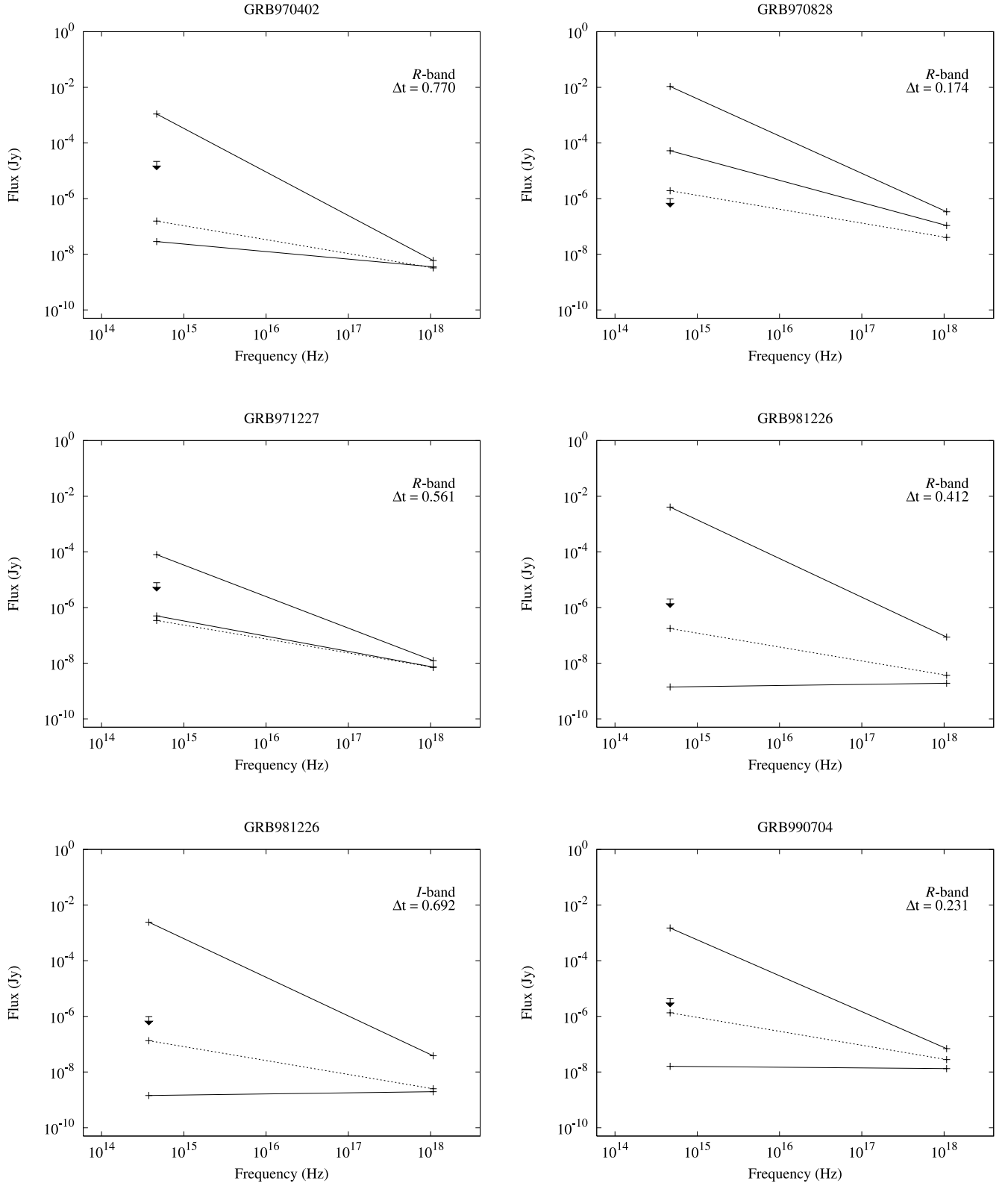
FIG. 1.—Ranges obtained for the optical counterpart fluxes for all GRBs in Table 1, by extrapolation of their X-ray measurements to the epoch and frequency of their optical upper limits; these limits are indicated by a downward-pointing arrow. The solid lines show the two extreme extrapolations, within which an optical counterpart should be found: the bottom line was obtained by extrapolating the $-1\,\sigma$ X-ray flux according to the lowest possible temporal and spectral slopes, and the top line was obtained by extrapolating the $+1\,\sigma$ X-ray flux using the highest possible temporal and spectral slopes. The dashed lines follow from extrapolating $-1\,\sigma$ X-ray flux with the lowest temporal and spectral slope with $p = 2$.

GRB990806

B-band
Δt = 0.667

GRB990806

R-band
Δt = 0.697

GRB991014

R-band
Δt = 0.467

GRB991014

K-band
Δt = 1.240

GRB000210

R-band
Δt = 0.686

GRB000214

R-band
Δt = 0.337

Fɪɢ. 1.—*Continued*

GRB000214

K-band
Δt = 1.350

GRB000528

R-band
Δt = 0.734

GRB000615

R-band
Δt = 0.188

GRB000615

H-band
Δt = 0.705

GRB001025A

R-band
Δt = 1.168

GRB001109

R-band
Δt = 0.375
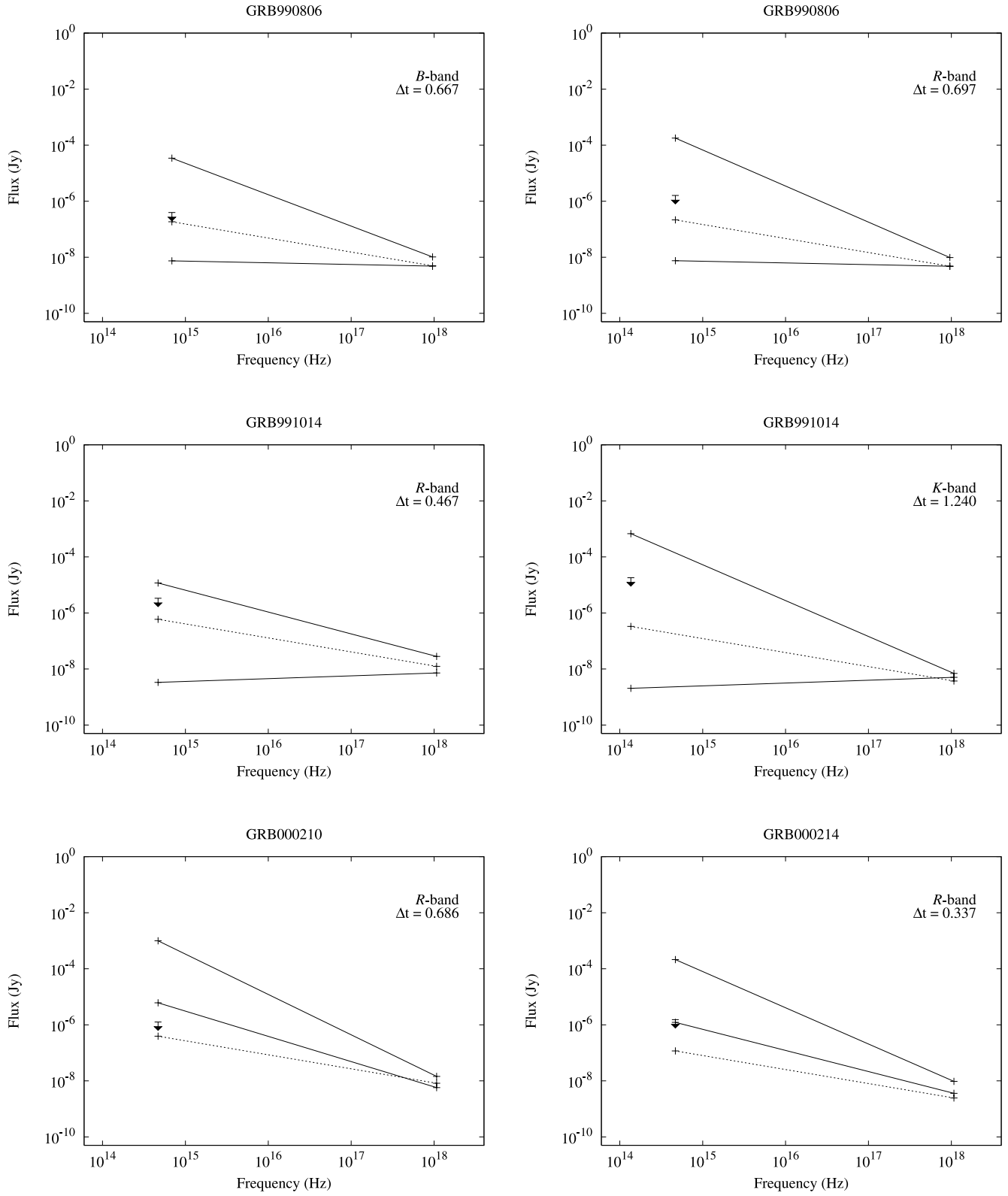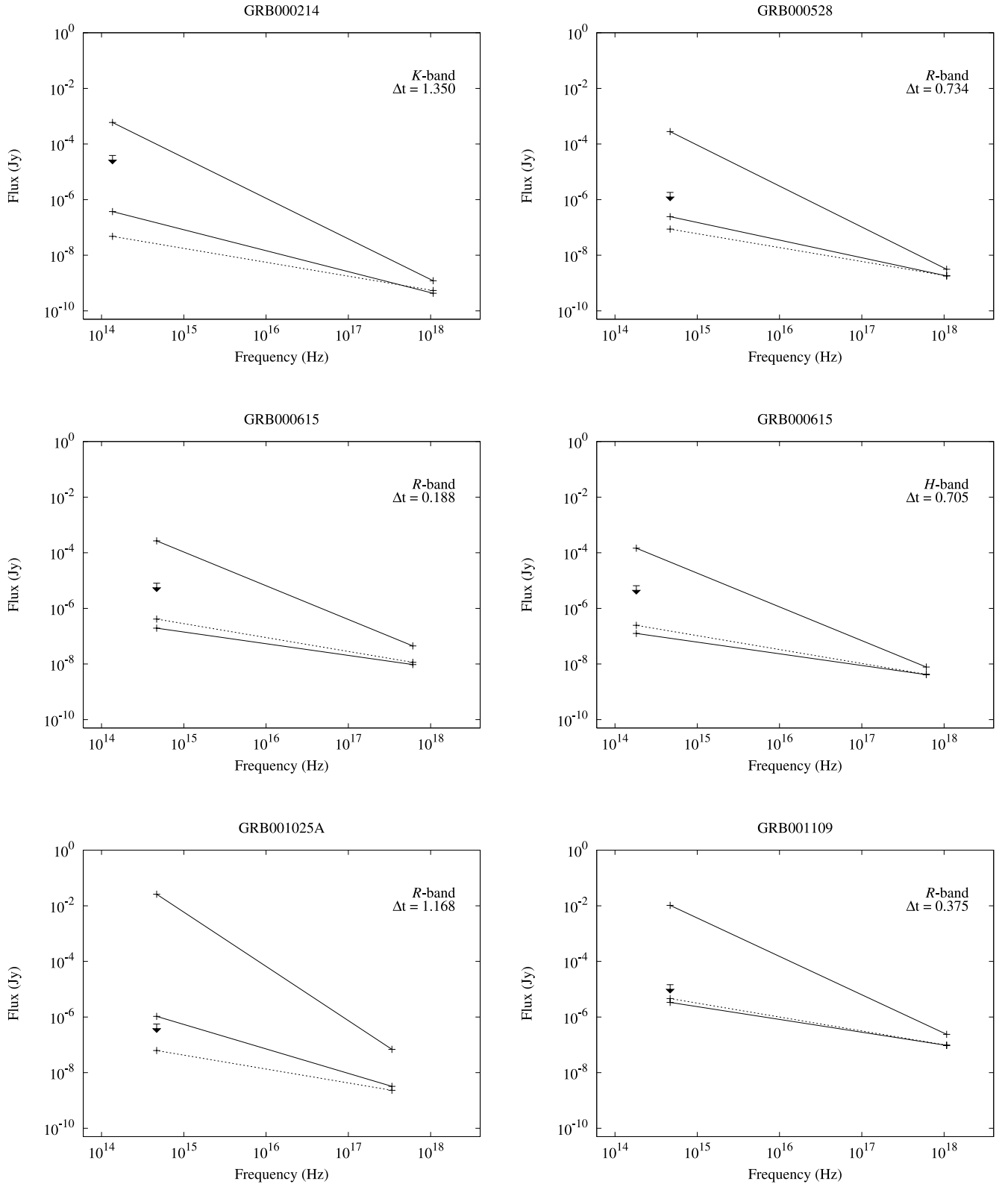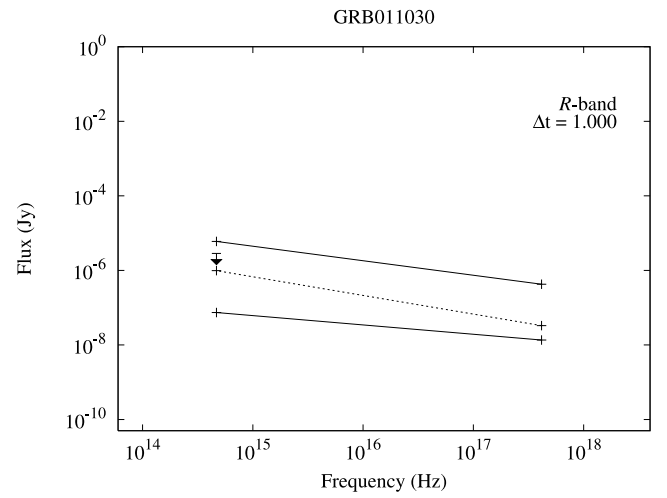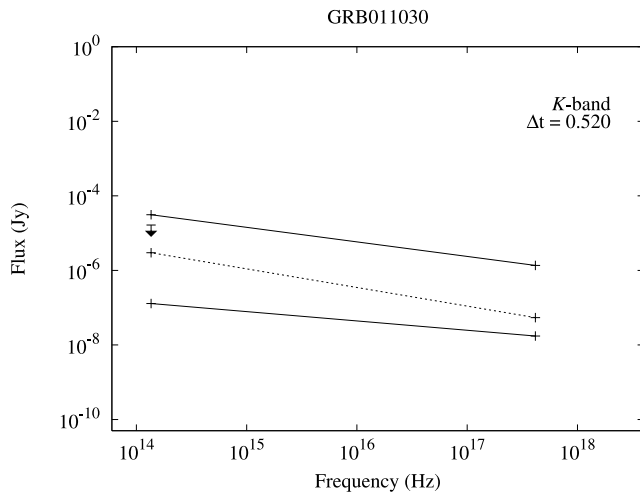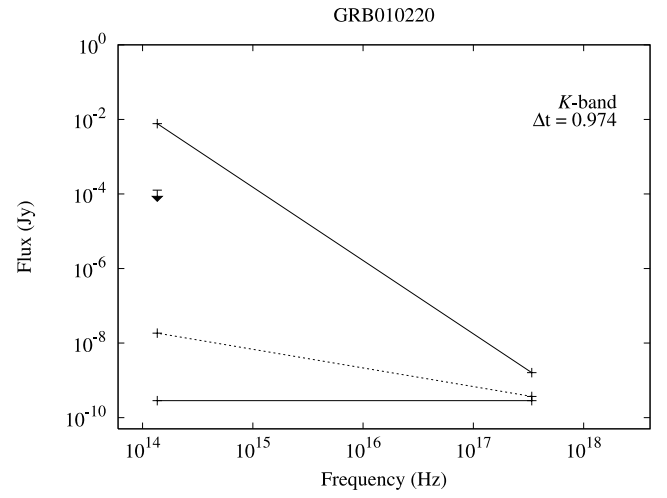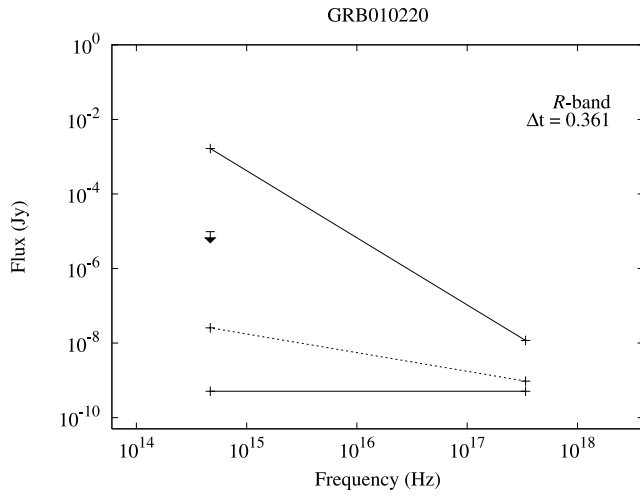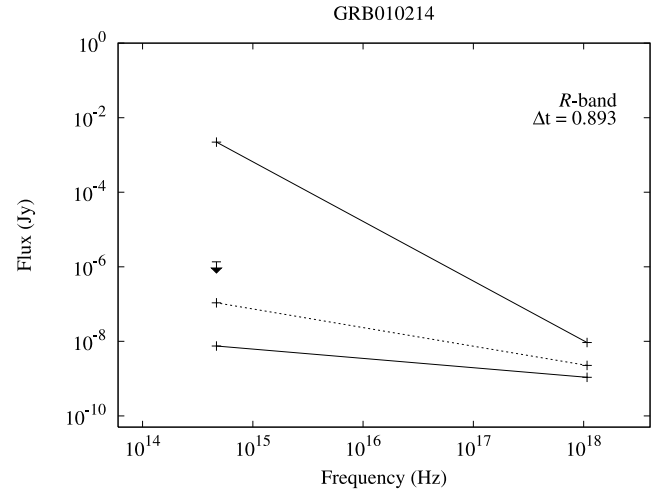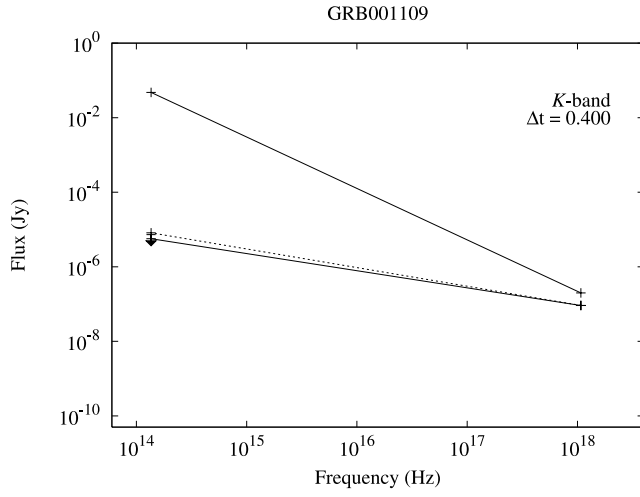
Fɪɢ. 1.—*Continued*

FIG. 1.—*Continued*
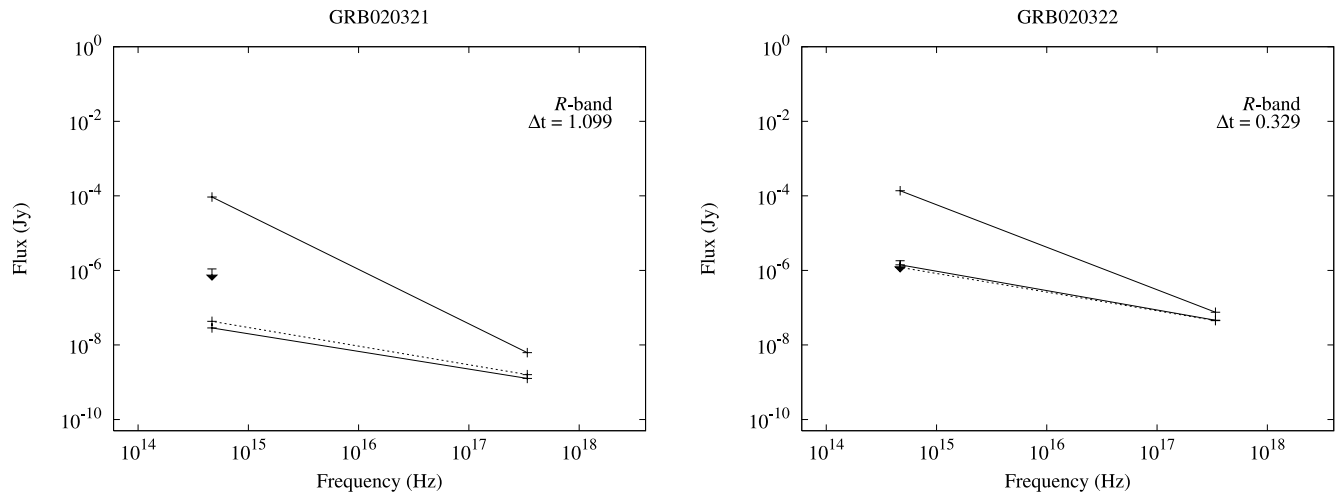
FIG. 1.—Continued

The validity of this division, particularly at early times, has to be investigated, but at the current moment the lack of early X-ray afterglows prevents the study of dark bursts at early times in two ways: (1) early X-ray afterglows will generally provide more accurate positions than the initial GRB position, which gives larger telescopes, which often have a smaller field of view, the possibility to concentrate on deep searches, and (2) early X-ray afterglows will prevent the increase in the error when extrapolating the X-ray afterglow in the time domain to its optical/near-IR upper limit. This lack will be amended with the early afterglows available from *Swift*.

Two bursts with an optical afterglow fall below this line, GRB 020322 and GRB 030115. For GRB 020322, the afterglow was detected at $R = 23.26$ (Bloom et al. 2002b) after the identification of the X-ray afterglow with *XMM-Newton* (Ehle et al. 2002). We have extrapolated the X-ray afterglow for this burst in the same way to its expected optical detection (see Fig. 1, *last panel*), and we find it to be compatible within the 1 σ range of the X-ray extrapolation. GRB 030115 was $R = 24.3$ 1 day after the burst and is very red, with an $R - K$ color of about 6 mag (Levan et. al. 2005). Therefore, it is likely that the burst suffers from large

extinction. Unfortunately, no X-ray afterglow has been reported for this burst.

The other upper limits below this line belong to (in time order) GRB 030324 (Moran et al. 2003) (first two upper limits), GRB 021113 (Levan et al. 2002), GRB 030324 (Moran et al. 2003), GRB 000615 (Stanek et al. 2000), GRB 990704 (Rol et al. 1999), GRB 000214 (this paper), GRB 001109 (Vreeswijk et al. 2000), GRB 981226 (Lindgren et al. 1999), GRB 990806 (Greiner et al. 1999; equivalent R-band magnitude), GRB 991105 (Palazzi et al. 1999), GRB 981226 (Bloom et al. 1998; equivalent R-band magnitude), and GRB 000830 (Jensen et al. 2000). Seven of these bursts (GRB 981226, GRB 990704, GRB 990806, GRB 991105, GRB 000214, GRB 001109, and GRB 000615) are included in our sample of analyzed afterglows and shown in Figure 1. For two of these (GRB 000214 and GRB 001109), the optical/near-IR limit is very close to the minimum extrapolation from X-rays, putting them at the border of physically defined gray/dark bursts. In fact, as this minimum extrapolation is an extreme possibility for the afterglow behavior, it would not be unreasonable to qualify GRB 000214 and GRB 001109 as dark bursts. However, to adhere to our definition of physically dark bursts, we choose not do so here.

4. DISCUSSION

Figure 2 shows that in an R magnitude versus time diagram, the physically defined dark bursts are located in a distinct region at the faint end of optically detected bursts. The detection of GRB 020322 and GRB 030115, whose magnitudes are comparable to the upper limits of the two dark bursts GRB 000210 and GRB 001025A, suggests that dark and detected bursts form a continuous group, rather than two clearly separated samples, and that the afterglows of most of the dark burst candidates might be found by deeper searches. Such afterglows may very well be highly reddened, as is the case for GRB 030115, and would require searches to be performed in the near-IR, rather than in the optical wavebands. One would expect that some dark bursts occupy the region of detected bursts; unfortunately, the X-ray data do not allow us to constrain the upper limits in this sample enough to find dark bursts in this region. Specifically, a well-defined spectral index will constrain the result of the X-ray extrapolation to optical/near-IR wavelengths. Such a constrained X-ray extrapolation, combined with an optical upper limit, can show whether physically dark bursts also occur in the upper part of Figure 2.
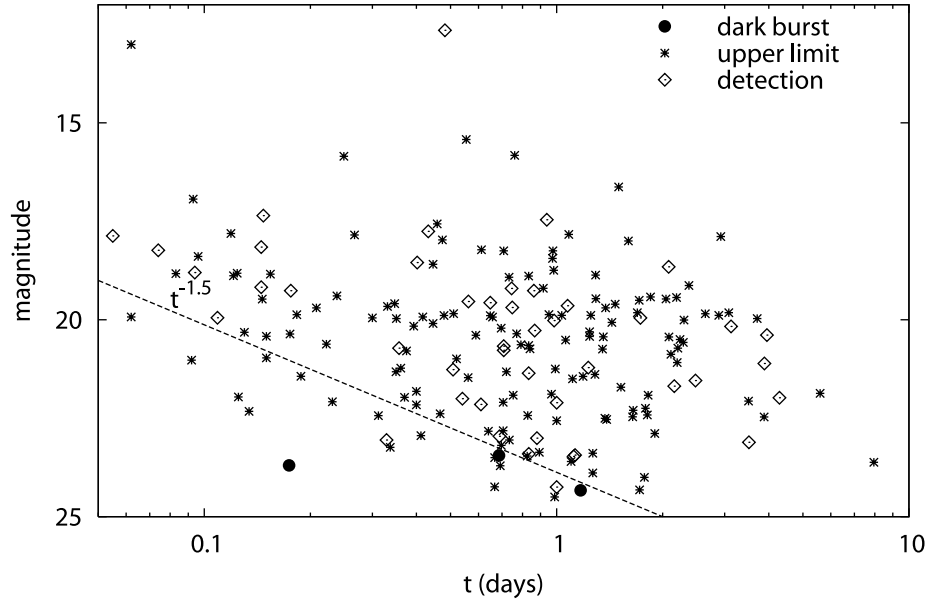
TABLE 4
Burst Classification and Amount of Host Galaxy Extinction
Inferred in the Observer Frame

Burst	Filters	Classification	Extinction (mag)
GRB 970402	R	Gray	. . .
GRB 970828	R	Dark	$\geq$4.304
GRB 971227	R	Gray	. . .
GRB 981226	R	Gray	. . .
GRB 990704	R	Gray	. . .
GRB 990806	B	Gray	. . .
GRB 991014	K, R	Gray	. . .
GRB 000210	R	Dark	$\geq$1.708
GRB 000214	K, R	Gray	. . .
GRB 000528	R	Gray	. . .
GRB 000615	H, R	Gray	. . .
GRB 001025A	R	Dark	$\geq$0.690
GRB 001109	K, R	Gray	. . .
GRB 010214	R	Gray	. . .
GRB 010220	K, R	Gray	. . .
GRB 020321	K, R	Gray	. . .

Fig. 2.—R magnitude vs. time diagram, containing all the R-band upper limits (asterisks) from Table 2, as well as all known detected afterglows (diamonds). For most afterglows, we have taken the first available R-band data point. The dark bursts listed in Table 4 are indicated by the three filled circles. The power law with $\alpha = -1.5$ indicates the region that separates the dark bursts from almost all detected afterglows.

More significantly, our method can be used as a diagnostic tool for the overall determination of dark bursts, provided that early X-ray and optical observations are available, to compare the calculation of the extrapolated values to the observed limits.

Here we speculate on three possible causes for the (physical) darkness: high-redshift bursts, different afterglow properties, and extinction within the host galaxy. However, we wish to note that our sample of three bursts is too small to draw any definite conclusions.

High-redshift bursts will go undetected at optical wavelengths because of extinction by the Lyα forest, although this would require an X-ray afterglow that is intrinsically much harder, as its redshifted flux is still detected in the 2–10 keV X-ray range. Furthermore, two dark bursts have a redshift from the detection of their host galaxy (GRB 970828 [$z = 0.9578$; Djorgovski et al. 2001] and GRB 000210 [$z = 0.846$; Piro et al. 2002]), which is well within the sample of detected afterglows and does not suggest a high-redshift origin for dark bursts. The redshifts of the two detected bursts with very dim afterglows, which fall within our region of dark bursts (GRB 020322 and GRB 030115), are not known. However, for GRB 030115 the possible host is visible at $R = 24.5$ (Garnavich 2003), putting its redshift at $z < 4.5$.

Dark bursts could form a subset of GRB afterglows with different afterglow properties. De Pasquale et al. (2003) have found that the X-ray fluxes of dark bursts are different from the X-ray fluxes of optically detected bursts. Their sample of dark bursts, however, is not physically defined as in this current study, but uses the observational definition, which includes nondetections that might be attributed to observing conditions.

To see whether there is anything remarkable in the prompt gamma-ray properties, we have compared the 40–700 keV gamma-ray fluences of the three physically dark bursts with a general set of bursts, obtained from the *BeppoSAX* GRBM data and the BATSE data (the BATSE 40–700 keV fluences were obtained from spectral fits to the BATSE archival data, while the GRBM data were obtained from literature). This comparison set was selected by choosing bursts for which narrow error boxes are available and have had optical follow-up campaigns,

to make the comparison set similar to the set of GRB data of the physically dark bursts. The set includes among others all the gray bursts. For GRB 001025A, the *Ulysses* 25–100 keV fluence was converted to the 40–700 keV range, using a conversion factor obtained by converting a set of 28 BATSE burst templates with known spectral shapes (see Bloom et al. 2001). The result is shown at the top of Figure 3. No obvious trend is visible, although we note that the dark bursts appear to have a higher than average 40–700 keV fluence. This is also noticeable in the bottom figure, where we have plotted the peak fluxes of the dark bursts together with those for a general sample of bursts: the three dark bursts are in the higher part of the sample. However, our set is too small to meaningfully apply any formal statistical test, and we note it here as a possible trend.

Such a correlation between the peak flux and the faintness of the optical afterglow could happen in the case of an external scenario for the GRB and its afterglow: if the prompt gamma-ray emission is the result of the interaction with an external medium instead of internal shocks, a higher density of the medium would then result in a higher gamma-ray peak flux of the burst. A higher density would, however, also result in a higher absorption depth (provided the path length is long enough) and the optical/UV emission would go undetected.

Extinction as a likely cause for dark bursts was already suggested by Groot et al. (1998) for GRB 970828. More recently, Klose et al. (2003) explored the available K-band upper limits of GRBs and also found evidence for extinction to explain dark bursts. The two dark bursts with an identified host galaxy have already been discussed before. GRB 970828 has one of the deepest early upper limits available, as well as a host galaxy and a redshift. Djorgovski et al. (2001) show that a possible dust lane or giant molecular cloud could provide the amount of extinction needed to obscure the afterglow. For GRB 000210, the X-ray spectrum shows significant N_H absorption; the amount of dust needed to obscure an optical afterglow at the redshift of the host galaxy is consistent with this column density. Both findings favor dust extinction in the host galaxy for these two dark bursts.
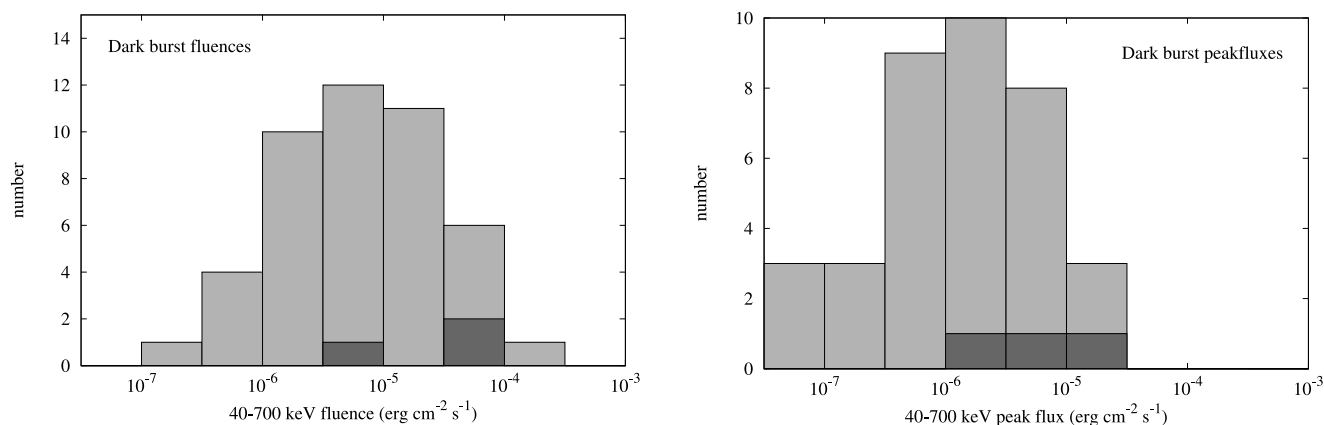
Fig. 3.—*Left:* Distribution of the dark burst fluences (40–700 keV) compared to those of a sample of nondark BATSE and *BeppoSAX* bursts. The dark burst histogram is indicated by the dark gray area. *Right:* Same as at left, but for the 40–700 keV peak fluxes.

Extinction should also be noticeable in optically detected bursts, and the $R - K$ color of 6 mag for GRB 030115 indeed suggests that this burst is heavily extincted. However, only very few bursts indeed show large extinction in the host galaxy. Even some notably faint afterglows, such as GRB 980613 (Hjorth et al. 2002) and GRB 000630 (Fynbo et al. 2001), have a low (<0.5 mag) extinction value in the R-band (in addition to Galactic extinction). It is therefore quite possible that we are simply not finding many heavily extincted bursts because these are still below the generally reported detection limits. However, the last 10 optical/near-IR follow-up campaigns of *HETE-2* SXC error boxes resulted in eight detected afterglows. This suggests that for the majority of the 60% of the cases where no afterglow was found for a *BeppoSAX* GRB, this was due to adverse observing conditions. Our sample and the SXC sample suggest a fraction of physically dark bursts more like 10%–20%. This may indicate that the few dark bursts we find here are indicative of the size of the actual (physical) dark burst sample.

5. CONCLUSIONS

The extrapolation from the X-ray afterglow to optical/near-IR wavelengths shows that only a very few bursts deserve the designation "dark burst." The optical upper limits obtained for these dark bursts are within a region at the fainter end of the optically detected bursts, with two optical afterglows found within this region. One of these two optical afterglows is highly reddened, which suggests that dark bursts can indeed be detected, albeit at very faint magnitudes. Detection of such dark bursts provides the necessary insights into the cause of their darkness.

Our method of extrapolation provides a useful diagnostic tool for setting a lower limit on the expected magnitude of the optical counterpart. When an early X-ray light curve and spectrum are available, for example from the XRT on board *Swift*, one can set a "dark burst upper limit." Any afterglow not detected above this upper limit is a potential candidate for a high redshift or an extinguished afterglow, or possibly even an afterglow produced by different physical mechanisms. Setting a search area using the currently available afterglow upper limits, as in

Figure 2, gives future afterglow searches a tool for picking out such potential dark bursts even without an X-ray afterglow.

It is, however, not possible to draw definite conclusions on the cause of darkness, owing to the small set of dark bursts we obtained. We note that in the gamma-ray properties, dark bursts appear to have higher than average fluences and peak fluxes, but we cannot statistically quantify this result yet. We also find that at least one burst showing large reddening (GRB 030115) is within the same region the of magnitude versus time diagram (Fig. 2) as the dark bursts.

Deep upper limits within 1 day, as well as early localizations and rapid follow-up observations, will complete and enhance Figure 2. The *Swift* mission can certainly help filling the gap for early times: it will provide early X-ray afterglow spectra and light curves, as well as rapid and precise localizations, needed for early (robotic) searches and deep searches with larger telescopes.

REFERENCES

Antonelli, L. A., et al. 1999, A&AS, 138, 435
———. 2000, ApJ, 545, L39
Beckwith, S., Evans, N. J., Becklin, E. E., & Neugebauer, G. 1976, ApJ, 208, 390
Berger, E., Frail, D. A., Price, P. A., Bloom, J. S., Galama, T. J., Kudritzki, R., & Bresolin, F. 2001, GCN Circ. 958, http://gcn.gsfc.nasa.gov/gcn/gcn3/958.gcn3

Berger, E., et al. 2002, ApJ, 581, 981
Bhattacharya, D. 2001, Bull. Astron. Soc. India, 29, 107
Bloom, J. S., Frail, D. A., & Sari, R. 2001, AJ, 121, 2879
Bloom, J. S., Gal, R. R., & Meltzer, J. 1998, GCN Circ. 182, http://gcn.gsfc.nasa .gov/gcn/gcn3/182.gcn3

Bloom, J. S., Kulkarni, S. R., & Djorgovski, S. G. 2002a, AJ, 123, 1111
Bloom, J. S., Mirabal, N., Halpern, J. P., Fox, D. W., & Lopes, P. A. A. 2002b, GCN Circ. 1294, http://gcn.gsfc.nasa.gov/gcn/gcn3/1294.gcn3
Castro Cerón, J. M., et al. 2004, A&A, 424, 833
Castro-Tirado, A. J., Gorosabel, J., Greiner, J., Zapatero-Osorio, M. R., & Costa, E. 1997, GCN Circ. 18, http://gcn.gsfc.nasa.gov/gcn3/018.gcn3
Chevalier, R. A., & Li, Z. 1999, ApJ, 520, L29
Costa, E., et al. 1997, Nature, 387, 783
———. 1998, BAAS, 193, 1372
De Pasquale, M., et al. 2003, ApJ, 592, 1018
Djorgovski, S. G., Frail, D. A., Kulkarni, S. R., Bloom, J. S., Odewahn, S. C., & Diercks, A. 2001, ApJ, 562, 654
Ehle, M., Rodriguez-Pascual, P., Loiseau, N., Santos-Lleo, M., Gonzalez-Riestra, R., Verdugo, E., Tomas, L., & Schartel, N. 2002, GCN Circ. 1293, http://gcn.gsfc.nasa.gov/gcn/gcn3/1293.gcn3
Feroci, M., et al. 2001, A&A, 378, 441
Frail, D. A., Kulkarni, S. R., Nicastro, S. R., Feroci, M., & Taylor, G. B. 1997, Nature, 389, 261
Frontera, F. 2003, in Supernovae and Gamma-Ray Bursters, ed. K. W. Weiler (Berlin: Springer), 317
Frontera, F., et al. 2000, ApJ, 540, 697
Fruchter, A., Krolik, J. H., & Rhoads, J. E. 2001, ApJ, 563, 597
Fukugita, M., Shimasaku, K., & Ichikawa, T. 1995, PASP, 107, 945
Fynbo, J. P. U., et al. 2000, GCN Circ. 867, http://gcn.gsfc.nasa.gov/gcn/gcn3/867.gcn3
———. 2001, A&A, 369, 373
Garnavich, P. 2003, GCN Circ. 1848, http://gcn.gsfc.nasa.gov/gcn/gcn3/1848.gcn3
Gorosabel, J., et al. 2000, GCN Circ. 783, http://gcn.gsfc.nasa.gov/gcn/gcn3/783.gcn3
Greiner, J., Pompei, E., Els, S., Pinfield, D., Brillant, S., Sterzik, M., Wolf, C., & Antonelli, A. 1999, GCN Circ. 396, http://gcn.gsfc.nasa.gov/gcn/gcn3/396.gcn3
Greiner, J., et al. 2000, GCN Circ. 887, http://gcn.gsfc.nasa.gov/gcn/gcn3/887.gcn3
Groot, P. J., et al. 1997, IAU Circ., 6616, 2
———. 1998, ApJ, 493, L27
Guidorzi, C., et al. 2003, A&A, 401, 491
Hjorth, J., et al. 2002, ApJ, 576, 113
———. 2003a, ApJ, 597, 699
———. 2003b, Nature, 423, 847
in 't Zand, J. J. M., et al. 2000, ApJ, 545, 266
———. 2004, in ASP Conf. Ser. 312, Gamma-Ray Bursts in the Afterglow Era: 3rd Rome Workshop, ed. M. Feroci et al. (San Francisco: ASP), 18
Jensen, B. L., Pedersen, H., Hjorth, J., Gorosabel, J., Fynbo, J. P. U., & Nowotny, W. 2000, GCN Circ. 788, http://gcn.gsfc.nasa.gov/gcn/gcn3/788.gcn3
Kemp, J., Uglesich, R., Mirabal, N., Halpern, J., Harkavy, D., & Costa, E. 1999, GCN Circ. 397, http://gcn.gsfc.nasa.gov/gcn/gcn3/397.gcn3
Klebesadel, R. W., Strong, I. B., & Olson, R. A. 1973, ApJ, 182, L85
Klose, S., et al. 2001, GCN Circ. 1142, http://gcn.gsfc.nasa.gov/gcn/gcn3/1142.gcn3
———. 2003, ApJ, 592, 1025
Lazzati, D., Covino, S., & Ghisellini, G. 2002, MNRAS, 330, 583
Levan, A. J., Kavelaars, J. J., Fruchter, A. S., & Rhoads, J. E. 2002, GCN Circ. 1688, http://gcn.gsfc.nasa.gov/gcn/gcn3/1688.gcn3
Levan, A. N., et al. 2005, ApJ, 622, 977

Li Causi, G., Di Paola, A., Antonelli, L. A., Puccetti, S., & Valentini, G. 2001, GCN Circ. 979, http://gcn.gsfc.nasa.gov/gcn/gcn3/979.gcn3
Lindgren, B., et al. 1999, GCN Circ. 190, http://gcn.gsfc.nasa.gov/gcn/gcn3/190.gcn3
Mészáros, P., & Rees, M. J. 1997, ApJ, 476, 232
Metzger, M. R., et al. 1997, Nature, 387, 878
Mohan, V., et al. 2001, GCN Circ. 1120, http://gcn.gsfc.nasa.gov/gcn/gcn3/1120.gcn3
Montanari, E., et al. 2001, in Gamma-ray Bursts in the Afterglow Era, ed. E. Costa, F. Frontera, & J. Hjorth (Berlin: Springer), 195
Moran, J., et al. 2003, GCN Circ. 2037, http://gcn.gsfc.nasa.gov/gcn/gcn3/2037.gcn3
Nicastro, L., et al. 1998, A&A, 338, L17
———. 2001, in Gamma-ray Bursts in the Afterglow Era, ed. E. Costa, F. Frontera, & J. Hjorth (Berlin: Springer), 198
Palazzi, E., et al. 1999, GCN Circ. 449, http://gcn.gsfc.nasa.gov/gcn/gcn3/449.gcn3
———. 2000, GCN Circ. 691, http://gcn.gsfc.nasa.gov/gcn/gcn3/691.gcn3
Panaitescu, A., & Kumar, P. 2001, ApJ, 560, L49
Pian, E., Masetti, N., Palazzi, E., Frontera, F., Ghinassi, F., Licandro, J., & Gandolfi, G. 2000, GCN Circ. 727, http://gcn.gsfc.nasa.gov/gcn/gcn3/727.gcn3
Piro, L., et al. 2002, ApJ, 577, 680
———. 1997, IAU Circ., 6617, 1
Rees, M. J., & Mészáros, P. 1992, MNRAS, 258, 41
Rhoads, J., Burud, I., Fruchter, A., Kouveliotou, C., & Wood-Vasey, M. 2001, GCN Circ. 1140, http://gcn.gsfc.nasa.gov/gcn/gcn3/1140.gcn3
Rhoads, J., Wilson, A., Storchi-Bergmann, T., & Fruchter, A. 2000, GCN Circ. 564, http://gcn.gsfc.nasa.gov/gcn/gcn3/564.gcn3
Rhoads, J. E. 1997, ApJ, 487, L1
———. 1999, ApJ, 525, 737
Rol, E., Salamanca, I., Kaper, L., Vreeswijk, P., & Tanvir, N., 2001, GCN Circ. 1059, http://gcn.gsfc.nasa.gov/gcn/gcn3/1059.gcn3
Rol, E., et al. 1999, GCN Circ. 374, http://gcn.gsfc.nasa.gov/gcn/gcn3/374.gcn3
Salamanca, I., et al. 2002, GCN Circ. 1385, http://gcn.gsfc.nasa.gov/gcn/gcn3/1385.gcn3
Sari, R., Piran, T., & Narayan, R. 1998, ApJ, 497, L17
Schlegel, D. J., Finkbeiner, D. P., & Davis, M. 1998, ApJ, 500, 525
Stanek, K. Z., Garnavich, P. M., Jha, S., & Berlind, P. 2000, GCN Circ. 709, http://gcn.gsfc.nasa.gov/gcn/gcn3/709.gcn3
Stanek, K. Z., et al. 2003, ApJ, 591, L17
Thorstensen, J., Uglesich, R., Halpern, J., Mirabal, N., Costa, E., Feroci, M., & Piro, L. 1999, GCN Circ. 423, http://gcn.gsfc.nasa.gov/gcn/gcn3/423.gcn3
Tiengo, A., Mereghetti, S., & de Luca, A. 2004, GCN Circ. 2548, http://gcn.gsfc.nasa.gov/gcn/gcn3/2548.gcn3
van Paradijs, J., et al. 1997, Nature, 386, 686
Vreeswijk, P., Rol, E., Packham, C., Tanvir, N., Kouveliotou, C., Wijers, R., & Knapen, J. 2000, GCN Circ. 886, http://gcn.gsfc.nasa.gov/gcn/gcn3/886.gcn3
Vreeswijk, P. M., et al. 2004, A&A, 419, 927
Watson, D., Reeves, J. N., Osborne, J. P., Tedds, J. A., O'Brien, P. T., Tomas, L., & Ehle, M. 2002a, A&A, 395, L41
Watson, D., et al. 2002b, A&A, 393, L1
Wijers, R. A. M. J., Rees, M. J., & Mészáros, P. 1997, MNRAS, 288, L51
Yoshida, A., et al. 2001, ApJ, 557, L27